INTERNATIONAL STANDARD

ISO 6980-2

Première edition
2004-10-15

Nuclear energy — Reference beta-particle radiation —

Part 2: Calibration fundamentals related to basic quantities characterizing the radiation field

Énergie nucléaire — Rayonnements bêta de référence —

Partie 2: Concepts d'étalonnage en relation avec les grandeurs fondamentales caractérisant le champ du rayonnement

Reference number
ISO 6980-2:2004(E)

PDF disclaimer

This PDF file may contain embedded typefaces. In accordance with Adobe's licensing policy, this file may be printed or viewed but shall not be edited unless the typefaces which are embedded are licensed to and installed on the computer performing the editing. In downloading this file, parties accept therein the responsibility of not infringing Adobe's licensing policy. The ISO Central Secretariat accepts no liability in this area.

Adobe is a trademark of Adobe Systems Incorporated.

Details of the software products used to create this PDF file can be found in the General Info relative to the file; the PDF-creation parameters were optimized for printing. Every care has been taken to ensure that the file is suitable for use by ISO member bodies. In the unlikely event that a problem relating to it is found, please inform the Central Secretariat at the address given below.

ISO copyright office
Case postale 56 • CH-1211 Geneva 20
Tel. + 41 22 749 01 11
Fax + 41 22 749 09 47
E-mail copyright@iso.org
Web www.iso.org

Published in Switzerland

Contents

Page

Foreword

ISO (the International Organization for Standardization) is a worldwide federation of national standards bodies (ISO member bodies). The work of preparing International Standards is normally carried out through ISO technical committees. Each member body interested in a subject for which a technical committee has been established has the right to be represented on that committee. International organizations, governmental and non-governmental, in liaison with ISO, also take part in the work. ISO collaborates closely with the International Electrotechnical Commission (IEC) on all matters of electrotechnical standardization.

International Standards are drafted in accordance with the rules given in the ISO/IEC Directives, Part 2.

The main task of technical committees is to prepare International Standards. Draft International Standards adopted by the technical committees are circulated to the member bodies for voting. Publication as an International Standard requires approval by at least 75 % of the member bodies casting a vote.

Attention is drawn to the possibility that some of the elements of this document may be the subject of patent rights. ISO shall not be held responsible for identifying any or all such patent rights.

ISO 6980-2 was prepared by Technical Committee ISO/TC 85, *Nuclear energy*, Subcommittee SC 2, *Radiation protection*. It is the second of a set of three standards concerning the production, calibration and use of beta-particle reference radiation fields for the calibration of dosemeters and dose-rate meters for protection purposes. The first standard in this series, ISO 6980-1 (being prepared), describes the methods of production and characterization of the reference radiation. The third standard in the series, ISO 6980-3 (being prepared), describes procedures for the calibration of dosemeters and dose-rate meters and the determination of their response as a function of beta energy and angle of incidence. This standard, the second in the series, supersedes ISO 6980:1996 and expands upon the calibration information provided in it. This standard describes procedures for the determination of absorbed-dose rate to a reference depth of tissue from beta-particle reference radiation fields.

ISO 6980 consists of the following parts, under the general title *Nuclear energy — Reference beta-particle radiation*:

— *Part 1: Method of production*

— *Part 2: Calibration fundamentals related to basic quantities characterizing the radiation field*

— *Part 3: Calibration of area and personal dosimeters and determination of their response as a function of energy and angle of incidence*

Nuclear energy — Reference beta-particle radiation —

Part 2: Calibration fundamentals related to basic quantities characterizing the radiation field

1 Scope

This part of ISO 6980 specifies methods for the measurement of the directional absorbed-dose rate in a tissue-equivalent slab phantom in the ISO 6980 reference beta-particle radiation fields. The energy range of the beta-particle-emitting isotopes covered by these reference radiations is 0,066 to 3,54 MeV (maximum energy). Radiation energies outside this range are beyond the scope of this standard. While measurements in a reference geometry (depth of 0,07 mm at perpendicular incidence in a tissue-equivalent slab phantom) with a reference class extrapolation chamber are dealt with in detail, the use of other measurement systems and measurements in other geometries are also described, although in less detail. The ambient dose equivalent, $H^*(10)$ as used for area monitoring of strongly penetrating radiation, is not an appropriate quantity for any beta radiation, even for that penetrating a 10 mm thick layer of ICRU tissue (i.e. $E_{\max} > 2$ MeV). If adequate protection is provided at 0,07 mm, only rarely will one be concerned with other depths, for example 3 mm.

This document is geared towards organizations wishing to establish reference-class dosimetry capabilities for beta particles, and serves as a guide to the performance of dosimetry with the reference class extrapolation chamber for beta-particle dosimetry in other fields. Guidance is also provided on the statement of measurement uncertainties.

2 Normative references

The following referenced documents are indispensable for the application of this document. For dated references, only the edition cited applies. For undated references, the latest edition of the referenced document (including any amendments) applies.

VIM:1993, *International Vocabulary of Basic and General Terms in Metrology,* second edition BIPM, IEC, IFCC, ISO, IUPAC, IUPAP, OIML

ISO 6980:1996, *Reference beta radiations for calibrating dosemeters and dose-rate meters and for determining their response as a function of beta-radiation energy*

ICRU 31:1979, *Average Energy Required to Produce an Ion Pair*

ICRU 37:1984, *Stopping Powers for Electrons and Positrons*

ICRU 39:1985, *Determination of Dose Equivalents Resulting from External Radiation Sources*

ICRU 44:1989, *Tissue Substitutes in Radiation Dosimetry and Measurement*

ICRU 51:1993, *Quantities and Units in Radiation Protection Dosimetry*

ICRU 56:1997, *Dosimetry of External Beta Rays for Radiation Protection*

3 Terms and definitions

For the purposes of this document, the terms and definitions given in ICRU Report 51, the International Vocabulary VIM:1993 and the following apply.

3.1
extrapolation curve
curve given by a plot of the corrected ionization current versus the extrapolation chamber depth

3.2
ICRU tissue
material with a density of 1 g·cm^{-3} and a mass composition of 76,2 % oxygen, 10,1 % hydrogen, 11,1 % carbon, and 2,6 % nitrogen (see ICRU Report 39)

3.3
ionization chamber
ionizing radiation detector consisting of a chamber filled with a suitable gas (almost always air), in which an electric field, insufficient to induce gas multiplication, is provided for the collection at the electrodes of charges associated with the ions and electrons produced in the measuring volume of the detector by ionizing radiation

NOTE The ionization chamber includes the measuring volume, the collecting and polarizing electrodes, the guard electrode, if any, the chamber wall, the parts of the insulator adjacent to the sensitive volume and any additional material placed over the ionization chamber to simulate measurement at depth.

3.3.1
extrapolation (ionization) chamber
ionization chamber capable of having an ionization volume which is continuously variable to a vanishingly small value by changing the separation of the electrodes and which allows the user to extrapolate the measured ionization density to zero collecting volume

3.4
ionization density
ratio of measured ionization per unit volume of air

3.5
leakage current
I_B
ionization chamber current measured at the operating bias in the absence of radiation

3.6
maximum beta energy
E_{max}
highest value of the energy of beta particles emitted by a particular nuclide which may emit one or several continuous spectra of beta particles with different maximum energies

3.7
parasitic current
I_p
negative current produced by beta particles stopped in the collecting portion of the collecting electrode and diffusing to this electrode and the wire connecting this electrode to the electrometer connector

3.8
phantoms
objects constructed to simulate the scattering and attenuation properties of the human body

NOTE In principle, the ISO water slab phantom, ISO rod phantom or the ISO pillar phantom should be used [19]. For the purposes of this standard, however, a polymethylmethacrylate (PMMA) slab, 10 cm × 10 cm in cross-sectional area by 5 cm thick, is sufficient to simulate the backscattering properties of the trunk of the human body, while tissue-equivalent materials such as polyethylene terephthalate (PET) are sufficient to simulate the attenuation properties of human tissue (see 5.2).

3.9
reference conditions
conditions which represent the set of influence quantities for which the calibration factor is valid without any correction

NOTE 1 The reference conditions for the quantity to be measured may be chosen freely in agreement with the properties of the instrument to be calibrated. The quantity to be measured is not an influence quantity.

NOTE 2 For the purposes of this International Standard, the reference values for temperature, atmospheric pressure and relative humidity are as follows:

— ambient temperature: $T_0 = 293{,}15$ K

— atmospheric pressure: $p_0 = 101{,}3$ kPa

— relative humidity: $r_0 = 0{,}65$

3.10
reference point of a dosemeter
point which is placed at the point of test for calibrating or testing purposes

NOTE 1 The point of test is the location of the reference point of the extrapolation chamber at which the conventionally true value is determined during calibration.

NOTE 2 The distance of measurement refers to the distance between the radiation source and the reference point of the dosemeter.

3.10.1
reference point of the extrapolation chamber
point to which the measurement of the distance from the radiation source to the chamber at a given orientation refers; the reference point is the centre of the back surface of the high-voltage electrode of the chamber

3.11
reference absorbed dose
D_{R}
personal absorbed dose, D_{p} (0,07), in a slab phantom made of ICRU tissue with an orientation of the phantom in which the normal to the phantom surface coincides with the (mean) direction of the incident radiation

NOTE 1 The personal absorbed dose D_{p} (0,07) is defined in ICRU Report 51. For the purposes of this standard, this definition is extended to a slab phantom.

NOTE 2 The slab phantom is approximated with sufficient accuracy by the material surrounding the standard instrument (extrapolation chamber) used for the measurement of the beta radiation field.

NOTE 3 D_{R} is approximated with sufficient accuracy by the directional absorbed dose in the ICRU sphere, D' (0,07, 0°).

3.11.1
reference beta-particle absorbed dose
$D_{\mathrm{R}\beta}$
reference absorbed dose, D_{R}, at a depth of 0,07 mm due only to beta particles

NOTE As a first approximation, the ratio $D_{\mathrm{R}\beta}/D_{\mathrm{R}}$ is given by the bremsstrahlung correction k_{br} (see C.3).

3.12
residual maximum energy
E_{res}
highest value of the energy of a beta-particle spectrum at the calibration distance after having been modified by scatter and absorption

3.13
standard test conditions
range of values of a set of influence quantities under which a calibration or a determination of response is carried out

NOTE 1 Ideally, calibrations should be carried out under reference conditions. As this is not always achievable (e.g. for ambient air pressure) or convenient (e.g. for ambient temperature), a (small) interval around the reference values may be used. The deviations of the calibration factor from its value under reference conditions caused by these deviations should, in principle, be corrected for. In practice, the uncertainty aimed at serves as a criterion to determine if an influence quantity has to be taken into account by an explicit correction or whether its effect may be incorporated into the uncertainty. During type tests, all values of influence quantities which are not the subject of the test are fixed within the interval of the standard test conditions.

NOTE 2 The range of values for ambient temperature, atmospheric pressure and relative humidity are as follows:

— ambient temperature: T = 291,15 to 295,15 K

— ambient pressure: p = 86 to 106 kPa

— relative humidity: r = 0,30 to 0,75

Working outside this range may result in reduced accuracy.

3.14
tissue equivalence
property of a material which approximates the radiation attenuation and scattering properties of ICRU tissue

3.15
transmission factor, $T_{\mathrm{m}}(\rho_{\mathrm{m}}\, d_{\mathrm{m}};\, \alpha)$
ratio of absorbed dose, $D_{\mathrm{m}}(\rho_{\mathrm{m}}\, d_{\mathrm{m}};\, \alpha)$, in medium m at an areal depth, $\rho_{\mathrm{m}}\, d_{\mathrm{m}}$, and angle of radiation incidence, α, to absorbed dose, D_{m} (0; 0°), at the surface of a phantom

3.15.1
tissue transmission factor, $T_{\mathrm{t}}(\rho_{\mathrm{t}}\, d_{\mathrm{t}};\, \alpha)$
ratio of absorbed dose, $D_{\mathrm{t}}(\rho_{\mathrm{t}}\, d_{\mathrm{t}};\, \alpha)$, in ICRU tissue at an areal depth, $\rho_{\mathrm{t}}\, d_{\mathrm{t}}$, and angle of radiation incidence, α, to absorbed dose, D_{t} (0; 0°), at the surface of an ICRU tissue slab phantom

3.16
zero point
reading of the extrapolation chamber depth indicator which corresponds to a chamber depth of zero, or no separation of the electrodes

4 Calibration and traceability of reference radiation fields

The reference absorbed-dose rate of a radiation field established for a calibration in accordance with this standard shall be traceable to a recognized national standard. The method used to provide this calibration link is achieved through utilization of a transfer standard. This may be a radionuclide source or an approved transfer standard instrument. The calibration of the field is valid in exact terms only at the time of the calibration, and thereafter must be inferred, for example, from a knowledge of the half-life and isotopic composition of the radionuclide source.

The measurement technique used by a calibration laboratory for calibrating a beta-particle measuring device shall also be approved as required by national regulations. An instrument of the same, or similar, type to that routinely calibrated by the calibration laboratory shall be calibrated by both a reference laboratory recognized by a country's approval body or institution, and the calibration laboratory. These measurements shall be performed within each laboratory using its own approved calibration methods. In order to demonstrate that adequate traceability has been achieved, the calibration laboratory should obtain the same calibration factor, within agreed-upon limits, as that obtained in the reference laboratory. The use by the calibration laboratory of standardized sources and holders which have been calibrated in a national reference laboratory is sufficient to guarantee traceability to the national standard.

The frequency of a field calibration should be such that there is reasonable confidence that its value will not move outside the limits of its specification between successive calibrations. The calibration of the laboratory-approved transfer instrument, and the check on the measurement techniques used by the calibration laboratory should be carried out at least every five years, or whenever there are significant changes in the laboratory environment or as required by national regulations.

For calibrations using beta-particle fields produced by radionuclide sources, traceability shall be provided either by using a radionuclide source whose reference absorbed-dose rate has been determined by a reference laboratory, or by determining the reference absorbed-dose rate at the instrument test position using an agreed-upon transfer instrument, calibrated at a reference laboratory.

5 General principles for calibrations of radionuclide beta-particle fields

5.1 General

Area and personal doses from beta-particle radiation are often difficult to measure because of their marked non-uniformity over the skin and variation with depth. In order to correctly measure the absorbed-dose rate at a point in a phantom in a beta-particle field, one needs a very small detector with very similar absorption and scattering characteristics as the medium of which the phantom is composed. Since there is no ideal detector, recourse shall be made to compromise both in detector size and composition. The concepts of “scaling factor” and “transmission factor” are helpful to account for these compromises.

5.2 Scaling to derive equivalent thicknesses of various materials

Scaling factors have been developed by Cross [1] to relate the absorbed dose determined in one material to that in another. These were developed from the observation that, for relatively high-energy beta-particle sources, dose distributions in different media have the same shape, differing only by a scaling factor, which Cross denoted as η. Originally observed in the comparison of beta ray attenuation curves in different media, where $\eta_{m,a}$, the scaling factor from medium m to air, was determined from the ratios of measured attenuation, the concept has been extended such that, for a plane source of infinite lateral extent, whether isotropic or a parallel beam, the absorbed dose at an areal depth $\rho_{m1}d_{m1}$ in medium m1 is related to the absorbed dose, in medium m2, at the same areal depth $\rho_{m2}d_{m2}$, but scaled to $\eta_{m1,m2}\rho_{m2}d_{m2}$, by

$$D_{m1}\left(\rho_{m1}d_{m1}\right) = \eta_{m1,m2}\cdot D_{m2}\left(\eta_{m1,m2}\ \rho_{m2}d_{m2}\right) = \eta_{m1,m2}\cdot D_{m2}\left(\eta_{m1,m2}\ \rho_{m1}d_{m1}\right) \quad (1)$$

provided that

$$\rho_{m1}d_{m1} = \rho_{m2}d_{m2} \quad (2)$$

$\eta_{m1,m2}$ is defined as the scaling factor from medium m1 to medium m2. It should be noted that the scaling factors are ratios, so that $\eta_{m1,m2} = 1/\eta_{m2,m1}$ and $\eta_{m1,m3} = \eta_{m1,m2}\eta_{m2,m3}$.

The user should be cautioned that this concept has been demonstrated only for materials of Z or effective atomic number, $\overline{Z}_m$, less than 18. Values of $\eta_{m,t}$ calculated for various materials relative to tissue are shown in Table 1 [2].

If we let m2 be tissue, and m1 be a medium m, Equation 1 reduces to

$$D_m\left(\rho_m\ d_m\right) = \eta_{m,t}\cdot D_t\left(\eta_{m,t}\ \rho_m d_m\right) \quad (3)$$

If we consider another depth, d'_m in medium m, one obtains a similar equation

$$D_m\left(\rho_m\ d'_m\right) = \eta_{m,t}\cdot D_t\left(\eta_{m,t}\ \rho_m d'_m\right) \quad (4)$$

The ratio of the absorbed dose at an arbitrary depth to that at the surface ($d'_{\mathrm{m}} = 0$) is defined as the transmission factor. Thus, making this substitution and dividing Equation 3 by Equation 4, we have

$$T_{\mathrm{m}}\left(\rho_{\mathrm{m}} d_{\mathrm{m}}\right) = \frac{D_{\mathrm{m}}\left(\rho_{\mathrm{m}} d_{\mathrm{m}}\right)}{D_{\mathrm{m}}(0)} = \frac{D_{\mathrm{t}}\left(\eta_{\mathrm{m,t}} \rho_{\mathrm{m}} d_{\mathrm{m}}\right)}{D_{\mathrm{t}}(0)} \tag{5}$$

or

$$T_{\mathrm{m}}\left(\rho_{\mathrm{m}}\ d_{\mathrm{m}}\right) = T_{\mathrm{t}}\left(\eta_{\mathrm{m,t}}\ \rho_{\mathrm{m}} d_{\mathrm{m}}\right) \tag{6}$$

The transmission through a layer of thickness of tissue, $\eta_{\mathrm{m,t}}\rho_{\mathrm{m}}d_{\mathrm{m}}$, in tissue is equal to the transmission through a layer of thickness of medium m, $\rho_{\mathrm{m}}d_{\mathrm{m}}$, in medium m. Thus the thickness $\rho_{\mathrm{m}}d_{\mathrm{m}}$ is said to be equivalent to tissue with a thickness of $\eta_{\mathrm{m,t}}\rho_{\mathrm{m}}d_{\mathrm{m}}$ since the transmissions are equal. We can define the equivalent tissue thickness $d_{\mathrm{t}}^{\mathrm{m}}$ as

$$d_{\mathrm{t}}^{\mathrm{m}} = \eta_{\mathrm{m,t}} \rho_{\mathrm{m}} d_{\mathrm{m}} \rho_{\mathrm{t}}^{-1} \tag{7}$$

In general the dose and the transmission factors are functions of both the depth and angle of incidence in a medium. When they are expressed as above with no angle given, the angle is to be taken as 0°.

5.3 Characterization of the radiation field in terms of penetrability

The transmission function, $T_{\mathrm{t}}(\rho_{\mathrm{t}} d;\ \alpha)$, is an important parameter of the beta-particle reference radiation field. Because of the finite thickness of all detectors used to measure absorbed-dose rate, it is necessary to characterize the radiation field in terms of penetrability before it can be properly calibrated. Since the energy fluence of the beta particles in a field changes as the beta particles penetrate the medium, the determination of the relative dose as a function of depth (or depth-dose function) in a medium shall be performed with a detector which is not sensitive to this change in energy fluence. For this reason, the relative depth-dose function shall be determined with a thin (2 mm or less) air ionization chamber. A recommended method for making this determination with the extrapolation chamber is given in reference [24]. The depth-dose functions are then used to construct transmission functions, examples of which are shown in Figure 1. The measured transmission functions, in conjunction with the calculated equivalent tissue thicknesses described above, can be used to determine corrections in the measured absorbed-dose rate to account for finite detector size and non-medium equivalence of the detector material. They can also be used to account for variations in the absorbed-dose rate at the reference point due to variations in the air density between the source and the reference point, and for attenuation in non-tissue material in front of the detector (see Annex C).

For thick detectors, one must account for the fact that the absorbed-dose rate is averaged over the volume of a detector. Neglecting any variation in the absorbed dose rate in the plane transverse to the normal direction of the field, the average absorbed-dose rate of a detector with a thickness v and density ρ, whose front surface is at a depth d in a phantom of unit density, is given by

$$\bar{D}_{\mathrm{m}}\left(d, v, \rho\right) = \frac{\int_{d}^{d+\rho v} D_{\mathrm{m}}\left(\delta\right) \mathrm{d}\delta}{\rho v} = \frac{D_{\mathrm{m}}\left(0\right) \int_{d}^{d+\rho v} T\left(\delta\right) \mathrm{d}\delta}{\rho v} = D_{\mathrm{m}}\left(0\right) \bar{T}\left(d, v, \rho\right) \tag{8}$$

For thick detectors ($v > 0{,}1$ mm), this effect may be compensated for by shifting the reference point towards the source from the centre of the detector.

6 Calibration procedures using the extrapolation chamber

6.1 General

The extrapolation chamber is the primary measurement device for specifying dose rate in beta-particle fields. It is a parallel plate chamber which consists of components which allow a variable ionization volume to be

achieved, by movement of one of the plates towards the other. A typical design [3] is shown in Figure 2, which utilizes a fixed entrance window and a movable collecting electrode. The entrance window also serves as the high-voltage electrode, and consists of a very thin conducting plastic foil. The window must be thin enough to not unduly attenuate the beta-particle radiation, yet strong enough to not be deformed by attraction to the grounded collecting electrode. Carbonized PET foils of about 0,7 mg · cm^{-2} are now typical of commercially available devices. The collecting electrode is maintained at ground potential and defines the cross-sectional area of the ionization volume. It must be of conducting material or have a conducting coating, and must be surrounded by, and electrically insulated from, a guard region. This insulation must be thin enough to not perturb the electric field lines in the chamber volume, which ideally are uniform, and everywhere perpendicular to the two electrodes. In the design shown in Figure 2, the collecting electrode is constructed from polymethylmethacrylate (PMMA) which has a thin coating of conductive material in which a narrow groove has been inscribed to define the collecting area. The device must be equipped with an accurate means to determine incremental changes in the distance between the two electrodes, hereafter referred to as the chamber depth; a micrometer attached to the piston which drives the collecting electrode is usually employed. A bipolar, variable voltage DC power source is used to supply the high voltage to the collecting electrode, and a low-noise electrometer is used to measure the current collected by the collecting electrode. Details of the measurement of the ionization current are given in Annex B.

6.2 Determination of the reference beta-particle absorbed-dose rate

The determination of the absorbed-dose rate to tissue due to beta particles measured with an extrapolation chamber is derived from the following general relationship:

$$\dot{D}_{\mathrm{t}} = \frac{\bar{W}_0}{e}\, s_{\mathrm{t,a}} \left[\frac{\Delta I}{\Delta m_{\mathrm{a}}} \right]_{\mathrm{BG}} \tag{9}$$

where ΔI is the increment of ionization current and Δm_{a} is the increment of the mass of air in the collecting volume under Bragg-Gray (BG) conditions. Unfortunately Bragg-Gray (BG) conditions are generally not realized in measurements of the beta-particle reference radiation fields, and to overcome this difficulty, various corrections are applied and the evaluation of the reference beta-particle absorbed-dose rate is accomplished with

$$\dot{D}_{\mathrm{R}\beta} = \frac{\left(\bar{W}_0 / e\right) s_{\mathrm{t,a}}}{\rho_{a0} \quad a} \left[\frac{\mathrm{d}}{\mathrm{d}\ell} \{kk' I(\ell)\} \right]_{\ell=0} \tag{10}$$

where

$\left(\bar{W}_0 / e\right)$ is the quotient of the mean energy required to produce an ion pair in air under reference conditions and the elementary charge e, with a recommended value of (33,83 ± 0,06) J C^{-1} [4,5] (this value may be used for standard test conditions without correction);

ρ_{a0} is the density of air at the reference conditions of temperature, pressure and relative humidity;

a is the effective area of the collecting electrode;

$\left[\frac{\mathrm{d}}{\mathrm{d}\ell} \{kk' I(\ell)\} \right]_{\ell=0}$ is the limiting value of the slope of the corrected current versus chamber depth ℓ function;

$s_{\mathrm{t,a}}$ is the ratio of the mean mass-electronic stopping powers in tissue to air;

k' is the product of the correction factors which are independent of the chamber depth;

k is the product of the correction factors which vary with the chamber depth.

The various correction factors are described in Tables 2 and 3, and methods for determining them are given in Annex C. Methods for determining the limiting slope are given in Annex B.10. The quantity $s_{t,a}$ is given by

$$s_{t,a} = \frac{\int_0^{E_{max}} (\Phi_E)_t \, (S/\rho)_{el,t} \, dE}{\int_0^{E_{max}} (\Phi_E)_t \, (S/\rho)_{el,a} \, dE} \tag{11}$$

where $(\Phi_E)_t$ is the spectrum of electrons at the reference point of the extrapolation chamber, $(S/\rho)_{el,t}$ is the mass-electronic stopping power for an electron with kinetic energy E in tissue-equivalent material and $(S/\rho)_{el,a}$ is the corresponding quantity for air. It is assumed that secondary electrons (delta rays) deposit their energy where they are generated so that they do not contribute to the electron fluence. The upper limit of the integrals is given by the maximum energy, E_{max}, of the beta particles in the fluence spectrum and the lower limit corresponds to the lowest energy in the spectrum, here indicated by a zero. In principle, this spectrum also includes any electrons set in motion by bremsstrahlung photons but these are usually of negligible importance.

Values for $s_{t,a}$ have been calculated [3] using Equation 11 for several beta-emitting radioisotopes, on the idealized assumption that the beta particles continuously dissipate their energy. Measurements of $(\Phi_E)_t$ were performed [5] using electron spectrometers [2,6]. These data were not corrected for backscattering loss (less than 10 % of the incident beta particles are not detected due to backscattering from the detector surface) or detector resolution. However, they can be used to calculate $s_{t,a}$ to a sufficiently good approximation since $(S/\rho)_{el,m}$ depends only slightly on beta-particle energy. For the averaging, the values of $(S/\rho)_{el,m}$ of Seltzer [2] were used; the results are shown in Table 4.

For the determination of reference absorbed-dose rate, a thickness of PET should be added to the front surface of the extrapolation chamber such that the total thickness including the window is 7,6 mg·cm^{-2}. This thickness of PET is equivalent to a thickness of 7 mg·cm^{-2} of tissue according to the scaling relation discussed in 5.2.

7 Calibrations with other measurement devices

7.1 Calibrations with thermoluminescence dosemeters

Thin (less than 25 mg·cm^{-2}) thermoluminescence dosemeters (TLDs) of materials with low atomic number, such as LiF, $Li_2B_4O_3$, $Mg_2B_4O_7$, or Al_2O_3, may be used successfully without correction for detector thickness for the calibration of beta-particle radiation fields for all but the lowest energies ($E_{max} < 200$ keV). For the best results, these systems should be calibrated in reference beta-particle radiation fields. However, adequate results can be obtained with absorbed-dose calibrations in high-energy photon beams under conditions of electronic equilibrium. It is possible to use thicker dosemeters without corrections for thickness if they are loaded with an opaque material to effectively limit the light emitted only to the dosemeter surface. If thicker dosemeters are used, then an independent means shall be used to determine the transmission function in the medium of interest in order to correct the dosemeter reading for volume averaging effects (see 5.3). Measurements of reference absorbed-dose rate should be performed with the centre of the dosemeter at a depth of 7 mg·cm^{-2} in a tissue-equivalent phantom.

7.2 Calibrations with thermally stimulated exo-electron emission dosemeters

Thermally or optically stimulated exo-electron emission from BeO can be used as a dosemeter for beta-particle radiation at all reference radiation energies of interest, because the low energy of the emitted exo-electrons limits their emission to only the very outer (100 nm or less) surface of the detector, thus making them effectively extremely thin. As with thermoluminescence dosemeters, they are best calibrated in reference beta-particle radiation fields.

7.3 Calibrations with ionization chambers

Thin (a few mm or less) fixed-volume parallel plate ionization chambers may be used to calibrate beta-particle radiation fields for all but the lowest energies ($E_{max} < 200$ keV). Thicker detectors are suitable for the highest

energies only ($E_{max} > 1$ MeV). If calibrated in reference beta-particle radiation fields, fixed-volume ionization chambers may be used as transfer instruments to establish traceability to national standards (see Clause 4). Measurements should be performed on a phantom if the chamber rear wall is not sufficiently thick (less than 1 cm) to provide full backscatter.

7.4 Calibrations with scintillator detectors

A number of detection systems have been developed for beta-particle dosimetry which employ scintillators as the sensitive detection elements. In the pulse-counting mode, these systems are quite sensitive and may be employed successfully for the higher energy beta-particle fields. However, the dimensions of the scintillator are an important determinant in the energy dependence of the response due to the volume effects described in 5.3. Thus, scintillator systems used to calibrate beta-particle radiation fields shall be calibrated in reference beta-particle radiation fields of the same type as they are to be employed. When used in the pulse-counting mode, particular care must be taken at higher absorbed-dose rates to account for possible counting losses due to pulse processing dead time.

8 Measurements at non-perpendicular incidence

Measurements at non-perpendicular incidence to determine the absorbed-dose rate as a function of angle of incidence may be performed both with the extrapolation chamber and with thin thermoluminescence or exo-electron dosemeters. When using the extrapolation chamber for these measurements, care must be taken to account for the angular dependence of some of the correction factors applied to the measured currents. The correction which is the most sensitive is the perturbation correction, which should be determined for each angle of interest using the method of Böhm [7]. When thin TLDs are employed, only the very thinnest detectors are suitable (effective thicknesses less than 25 µm) because of the complicated angular-dependant volume effects in thicker dosemeters [8].

9 Uncertainties

The calibration of a radiation field obtained with an instrument shall be accompanied by a statement of the uncertainty of the quoted value. In the determination of this value, all the uncertainties of all the measurements and factors which contribute to the quoted value shall be assessed. The assignment of values to these uncertainties [9,10] may either be based on statistical methods (Type A) or by other means (Type B). For both types of assessment, the uncertainties are quoted as standard uncertainties. Type A standard uncertainties are estimated from the standard deviation (σ) of the mean that follows from an averaging procedure or an appropriate regression analysis.

In general, measurements may be in error in two ways: there may be a constant difference between the measured quantity and the true quantity (offset) and/or there may be a difference between the measured quantity and the true quantity which is not constant, but dependent on either the magnitude of the quantity being measured and/or on other influencing quantities such as time or temperature (gain). For measurements with the extrapolation chamber which are carried out over a range of chamber depths from which a limiting slope is determined, the effects of gain errors are particularly significant. The measurements necessary for determination of absorbed-dose rate with the extrapolation chamber are those associated with setting up the instrument, and those associated with current collection at the various chamber depths. The set-up measurements include the following:

y_0 the distance between the source surface and the extrapolation chamber reference point;

z the distance perpendicular to the beam axis between the centre of the extrapolation chamber and the beam axis, ideally 0;

α the angle between the beam axis and the extrapolation chamber axis, ideally 0;

d_{PET} the thickness of the entrance window plus material added to make a thickness equivalent to 7 mg·cm^{-2};

9

C the capacitance of the electrometer feedback capacitor;

a the effective area of the collecting electrode.

The measurements associated with current collection are the following:

ℓ the chamber depths;

U_1, U_2 the voltages induced on the feedback capacitor by the collected current;

t the integration time between the measurement of U_1 and U_2;

T the ambient temperature;

p the ambient atmospheric pressure;

r the ambient relative humidity;

$t_m - t_0$ the time between the measurement and the reference time;

U the polarizing voltage.

Each of these measurements can, in principle, be subject to uncertainties due to both offset and gain, and a knowledge of these shall be included in the full analysis of uncertainty (see Annex D).

In addition, the uncertainties due to the application of the various correction factors discussed in Annex C shall be considered, and in particular the effect of the uncertainties on the limiting slope. Methods for making such an assessment are discussed in Annex D. The uncertainties associated with the various components of Equation 10 (see 6.2) are shown in Table 6, with references to where uncertainties for the various quantities were obtained.

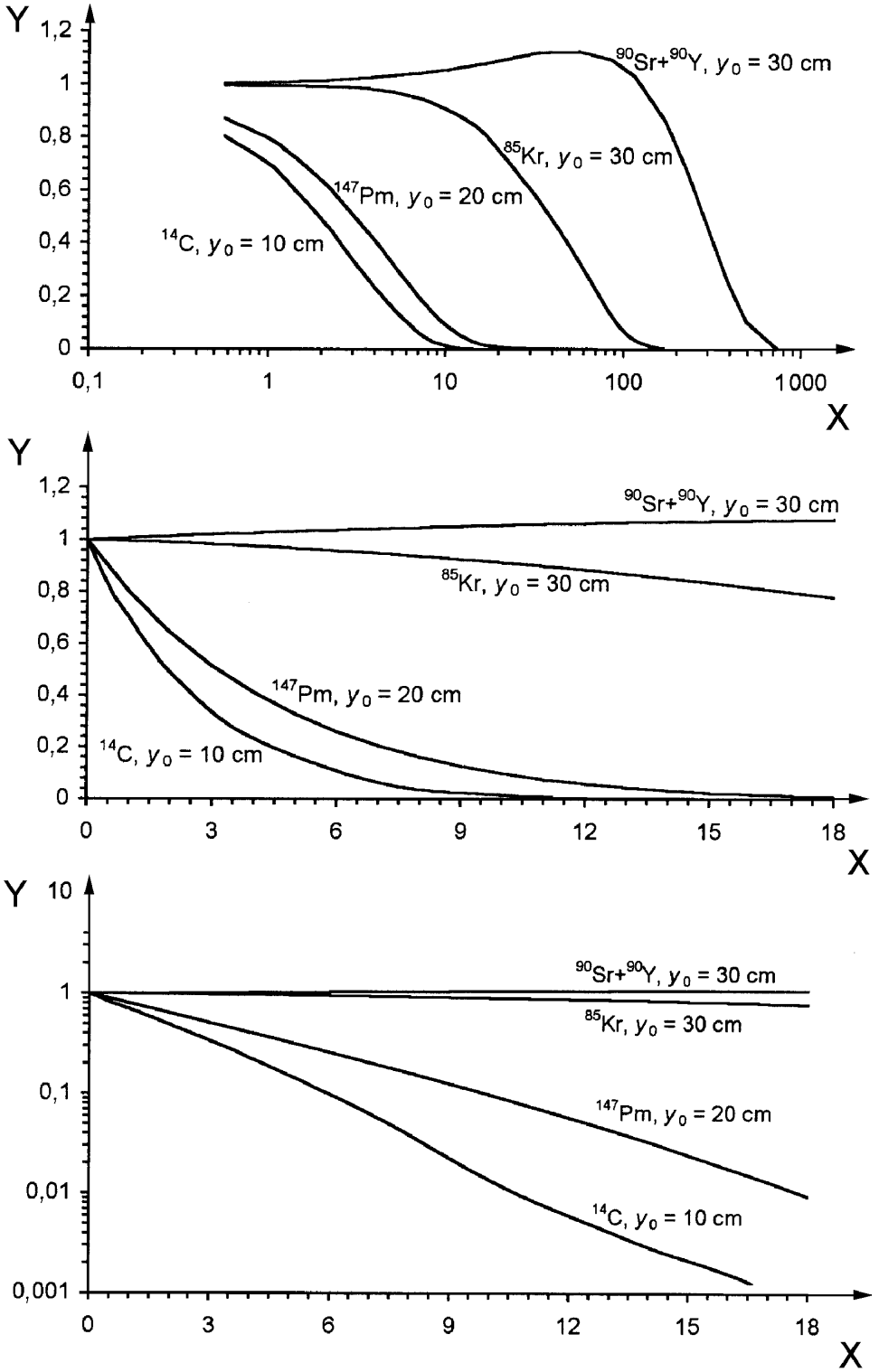

Key

X Tissue depth, mg·cm^{-2}

Y Transmission factor

Upper part: full depth dose curves with logarithmic scale for tissue depths.

Middle part: measured functions for tissue depths up to 18 mg·cm^{-2}.

Lower part: measured functions shown on a logarithmic scale for tissue depths up to 18 mg·cm^{-2}.

NOTE The depth dose curve for ^{204}Tl is very similar to that shown for ^{85}Kr.

Figure 1 — Depth dose curves measured at the calibration distances y_0 for several beta-particle sources

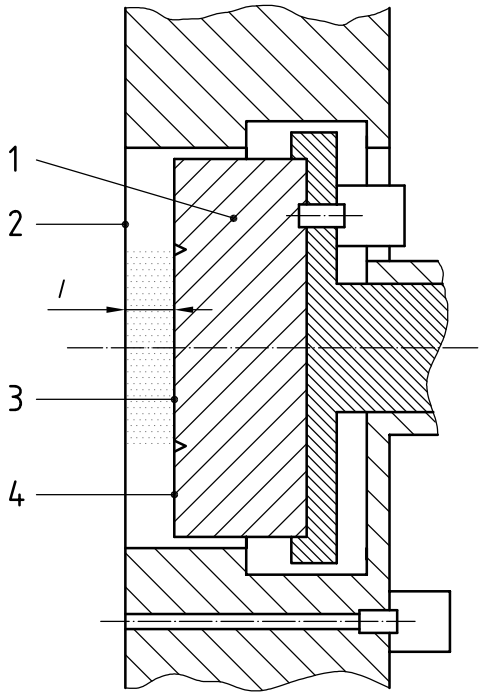

Key
1 piston
2 entrance window
3 collecting electrode
4 guard ring
ℓ chamber depth

Figure 2 — Schematic cross-section of the main parts of an extrapolation chamber

Table 1 — Calculated beta-particle scaling factors of low-Z media relative to tissue

Medium, m	$\eta_{m,t}$
A-150 plastic	0,983
Air	0,915
Aluminum	0,915
Aluminum oxide	0,908
Beryllium oxide	0,849
Calcium fluoride	0,958
Calcium sulfate	0,989
Carbon	0,875
ICRU tissue	1,000
Lithium fluoride	0,840
Lithium tetraborate	0,864
Magnesium tetraborate	0,883
Plastic scintillator (vinyltoluene based)	0,971
Polycarbonate	0,942
Polyethylene	1,012
Polyethylene terephthalate (PET)	0,933
Polyimide	0,916
Polymethylmethacrylate (PMMA)	0,963
Polystyrene	0,952
Polytetrafluoroethylene (PTFE)	0,884
Silicon	0,958
Skin	0,997
Water	1,015

Table 2 — Correction factors which are constant for the entire extrapolation curve measurement

Symbol	Description	Influencing parameters related to			
		Extrapolation chamber	Condition of use	Source	Irradiation conditions
k_{ba}	Correction factor for the difference in backscatter between tissue and the material of the collecting electrode	+		+	+
k_{br}	Correction factor for the effect of bremsstrahlung from the beta-particle source			+	
k_{el}	Correction factor for the electrostatic attraction of the entrance window due to the collecting voltage	+	+		
k_{hu}	Correction factor for the effect of humidity of the air in the collecting volume on the average energy required to produce an ion pair		+		
k_{in}	Correction factor for interface effects between the air in the collecting volume and the adjacent entrance window and collecting electrode	+			
k_{ra}	Correction for the radial non-uniformity of the beam, i.e. perpendicular to the beam axis	+			+

Table 3 — Correction factors which may vary during the extrapolation curve measurement

Symbol	Description	Influencing parameters relating to			
		Extrapolation chamber	Condition of use	Source	Irradiation conditions
k_{abs}	Correction factor for variations in the attenuation of beta particles between the source and the collecting volume due to variations from reference conditions	+		+	+
k_{ac}	Correction for the attenuation of beta particles in the collecting volume	+	+	+	
k_{ad}	Correction factor for the variations of the air density in the collecting volume from reference conditions		+		
k_{de}	Correction factor for the radioactive decay of the beta-particle source			+	
k_{di}	Correction factor for the axial non-uniformity of the beta-particle field	+		+	+
k_{pe}	Correction factor for the perturbation of the beta-particle flux density by the side walls of the extrapolation chamber	+		+	+
k_{sat}	Correction factor for ionisation losses due to ionic recombination	+	+		+

Table 4 — Calculated mean mass-electronic stopping power ratios

Value of $s_{t,a}$ for the radionuclide					Relative standard uncertainty (%)
^{14}C	^{147}Pm	^{204}Tl, ^{85}Kr	$^{90}Sr+^{90}Y$	$^{106}Ru+^{106}Rh$	
1,133	1,124	1,121	1,110	1,102	0,6

Table 5 — Examples of uncertainties (1 σ) **associated with the measurements necessary to determine absorbed-dose rate with the extrapolation chamber**

Correction factor or quantity	Unit	Reference for the quoted value	Method of evaluation of standard uncertainty	Values of the standard uncertainty for the radionuclides				
				^{14}C	^{147}Pm	^{204}Tl and ^{85}Kr	$^{90}Sr+^{90}Y$	$^{106}Ru+^{106}Rh$
y_0	mm		B	0,3				
z	mm		B	0,3				
α	degrees		B	0,1				
$\rho_{PET}d_{PET}$	$g \cdot cm^{-2}$		A	0,000 1				
C	pF		A-B	0,1				
a	cm^2	[3]	A-B	0,005				
ℓ	mm		B	0,001				
U_1	V		A	[a]				
			B	0,003				
U_2	V		A	[a]				
			B	0,003				
t	s		B	0,001				
T	K		B	0,1				
p	kPa		B	0,05				
r			B	0,02				
$t_m - t_0$	s		B	0,1				
U	V		B	0,1				

[a] The magnitude of the statistical uncertainty depends on the signal level.

Table 6 — Examples of uncertainties ($1\ \sigma$) associated with the parameters necessary to calculate absorbed dose from measurements with the extrapolation chamber

Correction factor or quantity	Unit	Values of the correction factor or quantity	Method of evaluation of uncertainty (A or B)	Values of the standard uncertainty for the radionuclides				
				^{90}Sr-^{90}Y	^{204}Tl; ^{85}Kr	^{147}Pm	^{14}C	^{106}Ru-^{106}Rh
$s_{t,a}$	—	1,110 – 1,133	B	0,007				
$\bar{W}_0 / e$	J·C^{-1}	33,83	B	0,068				
a	cm^2	7,251[b]	B	0,005				
ρ_{a0}	kg·m^{-3}	1,197 40	B	0,000 5				
I_+	fA	[a]	A – B	0,2 (A) and 0,4 (B)				
I_-	fA	[a]	A – B	0,2 (A) and 0,4 (B)				
ℓ	mm	0,25 – 2,5	B	0,001				
k_{ba}	—	1,0 – 1,01	B	0,003	0,003	0,004	0,004	0,003
k_{br}	—	0.995	B	0,002				
k_{el}	—	1	B	0,001				
k_{hu}	—	1		0,000 5	0,000 5	0,001	0,001	0,000 5
k_{in}	—	1	B	0,000 1				
k_{ra}	—	1,0 – 1,01	B	0,005				
slope dI/dℓ	fA·mm^{-1}	300	B	0,4	0,6	0,9	1,5	0,6
k_{abs}	—	0,84 – 1,25	B	0,003	0,002	0,006	0,008	0,002
k_{ad}	—	0,95 – 1,10	B	0,006				
k_{ac}	—	1,0 – 1,013	B	0,000 5		0,001	0,002	0,000 5
k_{de}	—	1	B	0,000 1	0,000 1	0,000 2	0,000	0,002
k_{di}	—	1,005	B	0,001				
k_{pe}	—	1,002	B	0,001				
k_{sat}	—	1,005	B	0,002				

[a] For values of I_+ and I_- between 5 fA and 400 0 fA.

[b] Typical value for a commonly used device.

Annex A
(informative)

List of symbols

a	effective area of the extrapolation-chamber collecting electrode
BG	Bragg-Gray conditions
B_{m}	backscatter factor, ratio of backscatter for medium m relative to that for air
C	external feedback capacitance
C_{k}	extrapolation chamber capacitance
c_{i}	coefficient of polynomial fitting functions
d_{m}	depth in a medium m
d_{t}	depth in ICRU tissue
$d_{\mathrm{t}}^{\mathrm{m}}$	tissue-equivalent thickness of medium m
d_0	reference depth in tissue of 0,07 mm
$D_{\mathrm{m}}(d_{\mathrm{m}})$	absorbed dose at a depth d_{m} in medium m
D_{R}	reference absorbed dose
$D_{\mathrm{R}\beta}$	reference beta-particle absorbed dose
$\tilde{D}(z,\varphi)$	relative absorbed dose measured at (z,φ) in a plane perpendicular to the beam axis
$\bar{D}\ (d_{\mathrm{m}},v,\rho_{\mathrm{m}})$	volume-averaged dose in a detector of thickness v, density ρ_{m} at depth d_{m}
$D_{\mathrm{p}}(d)$	personal absorbed dose at depth d in ICRU tissue
$D'(d;\ \vec{\Omega}\ )$	directional absorbed dose at depth d, on a radius having direction $\vec{\Omega}$
E	electron kinetic energy
E_1	constant in the saturation correction equation
E_{max}	maximum kinetic energy of a beta-particle spectrum
E_{res}	residual maximum energy of a beta-particle spectrum
e	charge of an electron
f_{i}	coefficients used for the calculation of k_{pe} and $T_{\mathrm{t}}'(\rho_{\mathrm{t}}d_{\mathrm{t}};\ \alpha)$
$H_{\mathrm{p}}(d)$	personal dose equivalent at depth d in ICRU tissue
$H'(d;\vec{\Omega}\ )$	directional dose equivalent at depth d, on a radius having direction $\vec{\Omega}$
ICRU	International Commission on Radiation Units and Measurements
ISO	International Organization for Standardization
k	product of the extrapolation chamber correction factors which vary during the extrapolation curve measurement
k'	product of the extrapolation chamber correction factors which are constant during the extrapolation curve measurement

k_{abs}	correction factor for variations in the attenuation and scattering of beta particles between the source and the collecting volume due to variations from reference conditions
k_{ac}	correction factor for attenuation of beta particles in the collecting volume
k_{ad}	correction factor for the variations of air density in the collecting volume from reference conditions
k_{ba}	correction factor for the difference in backscatter between tissue and the material of the collecting electrode and guard ring
k_{br}	correction factor for the effect of bremsstrahlung from the beta-particle source
k_{de}	correction factor for radioactive decay of the beta particle source
k_{di}	correction factor for axial non-uniformity due to divergence of the beta particle field
k_{el}	correction factor for electrostatic attraction of the entrance window due to the collecting voltage
k_{hu}	correction factor for the effect of humidity of the air in the collecting volume on $\bar{W}_0$
k_{in}	correction factor for interface effects between the air of the collecting volume and the adjacent entrance window and collecting electrode
k_{pe}	correction factor for perturbation of the beta-particle flux density by the side walls of the extrapolation chamber
k_{ra}	correction factor for radial non-uniformity of the absorbed dose rate in the beam
k_{sat}	correction factor for ionisation collection losses due to ionic recombination
k^*	Boltzmann's constant
ℓ	extrapolation chamber depth, the air gap between the collecting electrode and the entrance window
ℓ_0	intercept of the extrapolation curve with the chamber depth axis
m_a	mass of the air in the collecting volume of an extrapolation chamber
p	ambient atmospheric pressure
p_0	reference atmospheric pressure
PMMA	polymethylmethacrylate
PET	polyethylene terephthalate
q_m	measured ionization density
r	ambient relative humidity
r_0	reference relative humidity
$(S/\rho)_{el,m}$	mass-electronic stopping power in medium m
$s_{t,a}$	quotient of mass-electronic stopping powers of ICRU tissue and air
T	ambient air temperature
T_0	reference air temperature
$T_m(\rho_m d_m;\ \alpha)$	transmission factor $D_m(\rho_m d_m;\ \alpha)/D_m(0;\ 0°)$ in medium m
$T_t(\rho_t\ d_t;\ \alpha)$	transmission factor $D_t(\rho_t\ d_t;\ \alpha)/D_t(0;\ 0°)$ in tissue
$T_t'(\rho_t\ d_t;\ \alpha)$	specially normalized transmission factor $D_t(\eta_{a,t}\,\rho_a\,y_0 + \eta_{m,t} d_m \rho_m;\ \alpha)/D_t(\eta_{a,t}\rho_{a0}\ y_0 + \rho_t\ d_0;\ \alpha)$ in tissue
t	integration time for a current measurement

t_m	time at which a measurement is performed
t_0	reference time to which measurements are corrected to account for radioactive decay
$t_{1/2}$	half life of a radioisotope
U	absolute value of the collecting voltage in the extrapolation chamber
U_1, U_2	initial and final voltages on the feedback capacitor charged by current from the extrapolation chamber
v	thickness of a detector
$\bar{W}_0$	average energy to produce an ion pair in air under reference conditions
x_c	diameter of the geometric collecting electrode area
x_g	width of the insulating gap between the collecting and guard electrodes
y_0	distance from the source to the reference point of the detector
z	distance from the beam axis, perpendicular to that axis
$\bar{Z}_m$	effective atomic number of medium m
α	angle between the direction of the beam axis and the normal of the surface of the phantom
Γ_0	constant in the saturation-correction-factor equation
ε_a	dielectric constant for air
I	ionization current
I_L	leakage current, not induced by pre-irradiation of the chamber
I_{br}	ionization current caused by bremsstrahlung
I_p	parasitic current
I_+	current measured with positive polarity of collecting voltage
I_-	current measured with negative polarity of collecting voltage
$\eta_{m1,m2}$	beta-particle attenuation scaling factor of medium m1 relative to medium m2
ρ_a	density of air at ambient conditions
ρ_{a0}	density of air at reference conditions
ρ_m	density of medium m
ρ_t	density of ICRU tissue
σ	standard deviation
Φ_E	spectral distribution of beta-particle fluence
φ	angle in a plane perpendicular to the beam axis

Annex B
(normative)

Extrapolation chamber measurements

B.1 Electrometer warm-up and stability checks

Ideally the electrometer used for current measurements with the reference extrapolation chamber should be left powered continuously. If power is removed, the electrometer should be allowed to warm up and stabilize for at least 4 h when power is restored. Records should be kept on current measurements with standard beta-particle sources as quality checks on the overall current measurement system.

B.2 Determination of the leakage current

For measurements in geometries or with sources which result in low ionization currents in the extrapolation chamber (< 100 fA), the leakage current should be measured frequently to verify its magnitude and polarity dependence, if any. Preferably this should be accomplished with the source removed from the stand to remove the contribution to the leakage (see B.3) due to bremsstrahlung produced in the source shutter. For low activity (< 200 MBq) sources of ^{204}Tl or ^{147}Pm, it is often sufficiently accurate to leave the sources in place during these measurements, particularly when making measurements in an automated fashion for long integration times.

B.3 Measurements at both polarities

At each chamber depth, current measurements are made at both positive and negative polarities. This is because of the interaction of the beta-particle beam with the collecting electrode, which causes a negative current to be always superimposed upon the polarity-dependant ionization current. If the current measured at positive polarity is denoted by I_+ and that measured at negative polarity as I_-, then the current due to ionization in the chamber volume is given by

$$I = (I_+ - I_-) / 2 \qquad \text{(B.1)}$$

This equation assumes

— that the parasitic current I_p, is independent of the polarity,

— that any additional non-source induced currents, such as from leakage or electrical background, hereafter referred to as leakage current, I_L, are also independent of polarity of the collecting voltage, and

— that any other disturbing currents due to radiation-induced leakage or ionization produced by bremsstrahlung or beta particles in the air of the preamplifier, or in small air gaps in close vicinity to the wire connecting the collecting electrode to the preamplifier, can be neglected.

For low-level beta-particle sources, special precautions must be taken to assure that the leakage current is relatively constant and independent of polarity. It should be noted that the sum of the parasitic and leakage currents can be determined from

$$I_p + I_L = (I_+ + I_-) / 2 \qquad \text{(B.2)}$$

if the leakage current varies only slowly in time and is independent of polarity. Slight increases in the parasitic current are to be expected with decreasing air gaps. Variations from this behaviour are symptomatic of

problems associated with variable leakage current; thus the parasitic current is a useful quality control parameter.

In the case of the leakage current being dependent upon the polarity of the collecting voltage, then I_+ and I_- shall be separately corrected for leakage.

B.4 Voltage gradient

Since some corrections to the measured current, such as recombination, are functions of the voltage gradient, it is recommended that a constant voltage gradient be used at each chamber depth. This involves changing the high voltage every time the chamber depth is changed. The choice of the gradient employed is governed by the desire to keep the recombination at a minimum, yet to not cause deformation of the high-voltage electrode by attraction to the collecting electrode, or to exceed the level at which ion multiplication occurs. A voltage gradient of 10 $V \cdot mm^{-1}$ is recommended to achieve these ends.

B.5 Choice of chamber depths

A range of chamber depths should be chosen so as to uniquely specify the slope of the extrapolation curve. The smallest air gap should be chosen as close to zero as possible, yet large enough that the current is measurable. At least five air gaps should be chosen, which span a range over which the measured current is linear with the chamber depth. The smallest air gap should be no greater than 0,5 mm, while the largest should be no greater than 2,5 mm. A recommended choice of air gaps is from 0,25 to 2,5 mm in increments of 0,125 mm.

B.6 Modes for measurement of current

The external capacitor feedback mode is recommended over the direct measurement of current on an ampere scale, because of the greater sensitivity and reading accuracy of this method. To use this properly, the external capacitor needs to be accurately calibrated, and the integration time accurately known and controlled. The measured current is then given by

$$I_{+,-} = C(U_2 - U_1)/t \qquad \text{(B.3)}$$

where

C is the external capacitance (including that due to the electrometer);

t is the integration time;

U_1 and U_2 are the voltages measured by the electrometer in external feedback mode at the beginning and end of the integration period.

B.7 Integration times

Integration times should be chosen commensurate with the measured signal level. Obviously for very low currents, longer integration times are necessary to average out fluctuations due to variations in the leakage current. Typical values of the leakage current are of the order of $\pm$ 0,5 fA, which for a source with a dose rate of 1 µGy/s, at a chamber depth of 0,25 mm, is about 10 % of the measured signal for an extrapolation chamber with a 30 mm collecting electrode diameter. A good rule of thumb is that integration times sufficient to collect at least 0,5 pC should be employed. Thus, for the example given above, an integration time of 100 s is recommended. While it is convenient to use the same integration time independent of chamber depth, it is often more efficient to vary the integration time as a function of chamber depth, using shorter integration times for larger chamber depths commensurate with the rule of thumb given above.

B.8 Replicate readings

There is always a necessity to perform repeated readings at each air gap and polarity to establish the statistical uncertainty of the measurement. In determining the number of necessary replicates, one must be concerned with the signal level and the effect of changing the polarity on the stability of the ionization chamber. For meaningful standard deviations, at least five, and preferably ten readings should be made at each polarity and each chamber depth. The polarity should be changed from positive to negative and back, at least twice during this procedure, to rule out instabilities introduced by polarity changes.

B.9 Determination of the zero point and the effective collecting electrode area

The zero point can be determined from an electrical measurement of the chamber capacitance in a capacitor bridge circuit. For this determination, measurements of the chamber capacitance are made at several chamber depths; the inverse of the measured chamber capacitance is then plotted versus the chamber depth indicator and least-squares fitted to a linear function. The intercept of this function with the x-axis indicates the zero point.

The temperature dependence of the zero point of an extrapolation chamber such as the one shown in Figure 2 has been determined [3] to be $(-3{,}3 \pm 0{,}1)\ \mu m \cdot K^{-1}$. This temperature dependence is due to differences in the thermal coefficients of expansion of the various components of the extrapolation chamber. It is thus important to keep temperature drifts during measurements with the extrapolation chamber to a minimum. A recommended [20] maximum range of temperatures during any one extrapolation measurement is 0,1 K.

The effective electrode diameter is regarded as the sum of x_c, the geometric collecting electrode diameter, and x_g, the width of the insulator between the collecting and guard electrodes (see Figure 2). If the collecting electrode is accessible for demounting and microscopic examination, these dimensions can be measured directly with a travelling or measuring microscope. If, however, the collecting electrode is not accessible, the effective collecting area can be determined electrically using the measurements of the chamber capacitance, C_k for several chamber depths described above. The capacitance for plane parallel circular electrodes with a guard ring is given by [11]

$$C_k = \frac{\varepsilon_a (x_c + x_g)^2 \pi}{4\ell} = \frac{\varepsilon_a a}{\ell} \tag{B.4}$$

where

ℓ_0 is the chamber depth;

ε_a is the dielectric constant for air, $8{,}859\ 78\ pF \cdot m^{-1}$.

If one plots the indicated chamber depth versus the inverse of the measured capacitance, one obtains a straight line which has a slope $1/\varepsilon_a a$ from which the effective collecting electrode area, a, can be determined.

B.10 Determination of the limiting slope

The quantity needed to calculate the absorbed dose from an extrapolation curve measurement is the limiting slope, which is given by $[\mathrm{d}\{kk'I(\ell)\}/\mathrm{d}\ell]_{\ell=0}$, where k is the product of the correction factors which vary during the measurement of the extrapolation curve, and k' is the product of those which are constant. The limiting slope is determined by least-squares fitting of the extrapolation curve to a polynomial function. If the correction factors comprising k are accurate, then in principle the currents have been corrected to a condition where they are directly proportional to the chamber depth, and the extrapolation curve is a straight line; in this case a first-order polynomial is sufficient, i.e.

$$kk'I(\ell) = c_0 + c_1\ell \tag{B.5}$$

where

c_1 is the limiting slope, and is independent of ℓ.

In this equation, c_0 is the intercept of the extrapolation curve with the current axis; the intercept with the chamber depth axis is ℓ_0, and is given by

$$\ell_0 = -c_0 / c_1 \tag{B.6}$$

and is the chamber depth indication at which the predicted ionization current is zero. Non-zero values of ℓ_0 are indicative of an error (non-zero offset) in the chamber depth indicator.

In the case where the correction factors comprising k are inaccurate or incomplete, the extrapolation curve will not be a straight line but will exhibit some curvature, which is most often negative or "sub-linear". This is often the case when the correction factors deviate appreciably from unity, as is the case for ^{147}Pm. In this case, it is more appropriate [2] to use a least-squares fitted second-order polynomial of the form

$$kk'I(\ell) = c_0 + c_1\ell + c_2\ell^2 \tag{B.7}$$

where

c_1 is the slope of the extrapolation where it intercepts the current axis. If $c_2 < 0$, then the function is sublinear (negative curvature), and ℓ_0 is given by

$$\ell_0 = \frac{-c_1 + \sqrt{c_1^2 - 4c_0c_2}}{2c_2} \tag{B.8}$$

While graphing the extrapolation curve with the fitted function superimposed is commonly done to evaluate the data visually, it is very useful to also make a graph of the $\Delta I / \Delta \ell$ values versus the corrected chamber depths. [12] This is an extremely sensitive tool to evaluate the linearity and also the quality of the fit. For linear functions, the evaluated slope, c_1, in this representation is a horizontal line. Even slight deviations from linearity are immediately apparent in this representation of the data.

Annex C
(normative)

Extrapolation chamber measurement correction factors

C.1 Type of correction

Corrections which are applied to the measured current are of two types: those which are constant during the measurement of the extrapolation curve and those which are dependent on the chamber depth or some other varying parameter. The correction factors are summarized in Tables 2 and 3. The determination of each of these correction factors is discussed in the following sections.

C.2 Correction for the difference in backscatter between tissue and the material of the collecting electrode and guard ring, k_{ba}

Some of the incident beta particles are backscattered into the collecting volume by the collecting electrode and adjoining parts of the guard ring. Ideally, the beta particles should be backscattered in the same way as if the collecting electrode and the guard ring consisted of tissue, but as the collecting electrode may consist of other materials, this difference must be corrected for (correction factor k_{ba}).

Variations in backscatter of a medium m relative to a reference medium such as air are quantified by a ratio, known as the backscatter factor. Measurements of backscatter factors B_m of PMMA, graphite and the almost tissue-equivalent substance M3 [13] relative to air were performed for secondary standard sources of the radionuclides $^{90}Sr+^{90}Y$ and ^{204}Tl by means of ultra-thin $CaSO_4$: Dy/Teflon thermoluminescence dosemeters [14]. The backscatter factors were all equal (about 1,10) within the experimental uncertainty (coefficient of variation of 2 % obtained from five measurements). The experimentally determined backscatter factor for ^{147}Pm was much closer to unity (0,99).

The uncertainties of the experimentally determined backscatter factors are so large that small differences in the B_m values of materials with slightly different effective atomic numbers $\bar{Z}_m$ [2] could not be recognized. A small difference in the atomic numbers can be considered by assuming that, in the first approximation, the absorbed-dose rate due to backscattered radiation is proportional to $\bar{Z}_m$. This means that the backscatter factors B_t and B_{PMMA} for tissue and PMMA are related by

$$B_t = 1 + (B_{PMMA} - 1)\bar{Z}_t / \bar{Z}_{PMMA} \qquad \text{(C.1)}$$

where

$\bar{Z}_t = 6{,}498$, and

$\bar{Z}_{PMMA} = 5{,}858$ are the effective atomic numbers of tissue and PMMA.

The correction factor k_{ba} is given by

$$k_{ba} = B_t / B_{PMMA} \qquad \text{(C.2)}$$

The experimentally determined values of B_{PMMA} and the values of k_{ba} calculated by means of Equations C.1 and C.2 are summarized in Table C.1. The relative standard uncertainty of k_{ba} is much lower than that of B_{PMMA} (about 2 %) because only the difference in backscatter of two substances with only slightly differing $\bar{Z}_m$ must be corrected.

C.3 Correction for the effect of bremsstrahlung from the beta-particle source, k_{br}

In addition to that caused by beta particles, a small part of the ionization current, I, is caused by bremsstrahlung emitted from the source. As the bremsstrahlung has a much greater penetrating ability than the beta-particle radiation, the ionization current I_{br} due to bremsstrahlung can be measured by means of an absorber of low atomic number (PMMA, PET) positioned in front of the entrance window of the extrapolation chamber, and just sufficiently thick to stop the beta-particle radiation but only slightly attenuate the bremsstrahlung. The correction factor k_{br} for bremsstrahlung is defined by the equation

$$k_{br}\, I = I - I_{br} \tag{C.3}$$

Bremsstrahlung generated by the beta particles in the absorber can be neglected.

The contribution of bremsstrahlung to the absorbed-dose rate may be important if the calibration is not related to $\dot{D}_t$ (0) but to $\dot{D}_t$ (0,07), and the ratio $\dot{D}_t$ (0,07)/$\dot{D}_t$ (0) is small, which is the case for the ^{14}C and ^{147}Pm sources [16]. Values for k_{br} are given in Table C.2.

C.4 Correction for the electrostatic attraction of the entrance window, k_{el}

The electrostatic attraction of a thin entrance window caused by the electric field in the collecting volume can be determined by measuring the chamber capacity versus the collecting voltage at a chamber depth of 2,5 mm. A deflection of $(2{,}2 \pm 1{,}2)$ µm was measured [3] at a field strength of 100 V·mm^{-1}. As all measurements are recommended to be performed at field strengths ten times lower, the electrostatic attraction can be neglected and thus the correction factor $k_{el} = 1$ can be assumed.

C.5 Correction for the effect of humidity of the air in the collecting volume on the average energy required to produce an ion pair, k_{hu}

This correction factor is applied to the recommended conventional value of the average energy required to produce an ion pair at reference conditions, $\bar{W}_0$, to account for the increase of this value when the relative humidity deviates below the standard test conditions. At present, it is specified at only a single value of $r = 0$, (dry air) as k_{hu} $(r = 0) = 1{,}004$ [5]. For standard test conditions, k_{hu} may be taken as unity with an estimated uncertainty of 0,1 % (1σ).

C.6 Correction for interface effects between the air in the collecting volume and the adjacent entrance window and collecting electrode, k_{in}

A graphited PMMA collecting electrode and a graphited PET entrance window, such as are employed in the extrapolation chamber shown in Figure 2, have somewhat lower effective atomic numbers than the air in the collecting volume. However, the disturbance of the secondary electron flux at these graphite-air interfaces can be neglected as was deduced by measurements [15,17] at a Sn-air interface, if the extrapolation chamber is operated at standard test conditions and at chamber depths larger than 0,5 mm. For chamber depths of 0,5 mm or less, there is no information available. Until more information is available, the correction factor for interface effects is considered to be $k_{in} = 1$, independent of the chamber depth employed.

C.7 Correction for the radial non-uniformity of the absorbed-dose rate in the beam, k_{ra}

Use of a 30 mm diameter of the collecting electrode area results in a measurement of absorbed-dose rate averaged over this area. The reference absorbed-dose rate, on the other hand, is specified on the axis of the beam. Thus, any non-uniformity perpendicular to the beam axis must be corrected for. The beam non-uniformity can be mapped, e.g. by a photographic film [18], TLDs or radiochromic film positioned

perpendicular to the beam axis in the plane of the reference point of the extrapolation chamber. This correction factor is denoted k_{ra} and can be calculated from

$$k_{ra} = [\tilde{D}(0,0^{o})\pi(x_c + x_g)^2]/[4\int_0^{2\pi} d\varphi \int_0^{(x_c+x_g)/2} \tilde{D}(z,\varphi)z\,dz] = \frac{\tilde{D}(0,0^{o})\pi(x_c + x_g)^2}{4\int_0^{2\pi} d\varphi \int_0^{(x_c+x_g)/2} \tilde{D}(z,\varphi)z\,dz} \quad \text{(C.4)}$$

where

$\tilde{D}(z,\varphi)$ is the relative dose determined from the field map.

When the ISO Series 1 reference radiations are used, $k_{ra} = 1$ can be assumed, with a standard uncertainty of 0,2 to 0,5 %.

C.8 Correction for the air density in the collecting volume, k_{ad}

The density of the air in the collecting volume of the extrapolation chamber influences the collected current because, for a constant absorbed-dose rate, it is proportional to the number of air molecules available to be ionized, which is itself proportional to the air density. Thus the measured ionization must be corrected to the air density at reference conditions.

To a good approximation, the density of air at ambient conditions, ρ_a can be expressed as [20]

$$\rho_a = \rho_{a0}\left[\frac{p}{100{,}726} - \frac{r}{114{,}2}\left(\frac{T}{T_0}\right)^{17{,}97}\right]\frac{T_0}{T} \quad \text{(C.5)}$$

where

T is the absolute temperature, expressed in K, of the air in the collecting volume;

p is the air pressure, expressed in kPa;

r is the relative humidity of the air, expressed as a fraction;

ρ_{a0} is the air density for the reference conditions which are defined for the following parameters:

$T_0 = 293{,}15$ K;

$p_0 = 101{,}325$ kPa;

$r_0 = 0{,}65$.

For these conditions:

$\rho_{a0} = 1{,}197\,40$ kg·m^{-3}

Equation C.5 is valid only for standard test conditions. The correction factor for the variations of the air density within the collection volume, k_{ad}, is then given by

$$k_{ad} = \frac{\rho_{a0}}{\rho_a} \quad \text{(C.6)}$$

C.9 Correction for variations in the attenuation and scattering of beta particles between the source and the collecting volume due to variations from reference conditions, k_{abs}

The reference thickness of the entrance window of the extrapolation chamber is $d_0 = 0{,}07$ mm of ICRU tissue, or an areal density of 7 mg·cm^{-2}. The reference thickness of the air layer between the source and the surface of the extrapolation chamber is y_0 at the reference conditions or an air density of ρ_{a0}. Using Equation 7, this air thickness corresponds to a tissue depth of $\eta_{a,t}\rho_{a0}y_0\rho_t^{-1}$. Any deviation of the entrance window tissue-equivalent thickness from 0,07 mm, or ambient air density, ρ_a, from the reference air density, ρ_{a0} results in a different absorption of the beta radiation compared with reference conditions. The correction factor, k_{abs}, which accounts for this is given by

$$k_{abs} = 1/T_t'\left(\eta_{a,t}\rho_a y_0 + \eta_{m,t}d_m\rho_m; \alpha\right) \tag{C.7}$$

where

$\eta_{m,t}d_m\rho_m$ is the tissue-equivalent thickness of a window of medium m, thickness d_m and density ρ_m;

$T_t'(\rho_t\, d_t; \alpha)$ is a transmission function which is specially normalized to be unity for reference conditions.

For low-energy fields ($E_{max} < 200$ keV), these specially normalized functions are adequately represented by functions of the form

$$T_t'\left(\rho_t\, d_t, \alpha\right) = \exp\left[f_0(\alpha) + f_1(\alpha)\rho_t\, d_t + f_2(\alpha)\left(\rho_t\, d_t\right)\right]^3 \tag{C.8}$$

while for higher energy sources, functions of the form

$$T_t'\left(\rho_t d_t; \alpha\right) = f_3(\alpha) + f_4(\alpha)\,\rho_t d_t + f_5(\alpha)\left(\rho_t d_t\right)^2 \tag{C.9}$$

may be used. Values for these fitting parameters for some reference fields defined in ISO 6980:1996 are shown in Table C.3 for $\alpha = 0°$. These values were obtained as fits of measurements of transmission through thin PET foils [21].

C.10 Correction for the attenuation of beta particles in the collecting volume, k_{ac}

The average air layer in the extrapolation chamber volume corresponds to a tissue depth of $\eta_{a,t}\rho_{a0}(\ell/2)\rho_t^{-1}$ where ℓ is the chamber depth. The effect of this extra layer can be estimated from the transmission factor as

$$k_{ac} = T_t\left(\rho_t d_0 + \eta_{a,t}y_0\rho_{a0}; \alpha\right)/T_t\left(\rho_t d_0 + \eta_{a,t}\left[y_0 + \ell/2\right]\rho_{a0}; \alpha\right) \tag{C.10}$$

Attenuation of beta particles by the air in the collecting volume need only be considered for low energy sources such as ^{147}Pm. As this is a small correction factor, the ambient air density is approximated by the reference air density ρ_{a0}.

C.11 Correction for radioactive decay of the beta-particle source, k_{de}

The radioactive decay of the beta sources can be taken into account by the correction factor

$$k_{de} = \exp\left[\left(t_m - t_0\right)\ln(2)/t_{1/2}\right] \tag{C.11}$$

where

$t_{1/2}$ is the half-life of the radionuclide;

t_m is the time at which the measurement is made;

t_0 is the time to which the measurement is being corrected, which is the reference time for the measurement.

For the measurement of an extrapolation curve, the reference time is usually taken as the beginning of the measurement. Table C.4 shows values of half-lives for the most important beta-particle emitting nuclides [22].

C.12 Correction for axial non-uniformity, k_{di}

Axial non-uniformity of a beta-particle radiation beam is caused by the divergence of the radiation field due to the point-like nature of the source, and by attenuation in the phantom. The phantom is partly substituted by the air in the extrapolation chamber collecting and guard regions. The attenuation shall therefore be considered for air instead of phantom material.

The absorbed-dose rate in air, $\overline{\dot{D}_a}$, averaged over the collecting volume is calculated from $\dot{D}_a(y_0)$ at the entrance window by integration between y_0 and $y_0 + \ell$. If the variation of the absorbed-dose rate in air is assumed to obey the inverse square law over this short distance ℓ and its variation transverse to the beam neglected , then the average absorbed-dose rate in air is given by

$$\overline{\dot{D}_a} = \int_{y_0}^{y_0+\ell} \dot{D}_a(y_0)\frac{y_0^2}{y'^2}dy' \Big/ \int_{y_0}^{y_0+\ell} dy' = \dot{D}_a(y_0)\frac{y_0}{y_0+\ell} \tag{C.12}$$

where

y_0 is the distance from the source to the entrance window;

ℓ is the chamber depth.

Since the entrance window remains fixed as ℓ is varied, the axial non-uniformity correction factor is given by

$$k_{di} = \frac{\dot{D}_a(y_0)}{\overline{\dot{D}_a}} = 1 + \frac{\ell}{y_0} \tag{C.13}$$

C.13 Correction for the perturbation of the beta-particle flux density by the side walls of the extrapolation chamber, k_{pe}

The perturbation of the beta-particle flux density by the side walls of the extrapolation chamber has been studied in detail by Böhm [7]. The results show that the perturbation correction factor k_{pe} can be assumed to be the product of a shield factor and a scatter factor, the magnitudes of which depend on the chamber depth ℓ. k_{pe} can be determined by measurements of the ionization current with rings of varying thickness and of the same inner diameter as the chamber walls, with the rings positioned in front of the entrance window. This procedure simulates the addition of more wall material to the extrapolation chamber. For various chamber depths, the dependence of the ionization on the added wall thickness is measured, and the correction to zero wall thickness is determined by extrapolation of the measured data. Once this has been determined for a number of chamber depths, the numerical values of the correction factor k_{pe} may be fitted to a polynomial function of the chamber depth ℓ of the form:

$$k_{pe} = f_6 + f_7\ell + f_8\ell^2 \tag{C.14}$$

Examples of coefficients of such functions which can be used to calculate k_{pe} for various sources, determined using an extrapolation chamber of the type shown in Figure 2, are given in Table C.5.

C.14 Correction for ionization losses due to recombination, k_{sat}

A correction factor shall be applied to account for the losses in the collection of the ionization created in the chamber volume due to the effects of recombination. The three types of recombination, volume recombination, initial recombination and diffusion loss have been reviewed in detail by Böhm [23]. These effects are accounted for by the correction factor k_{sat}, which is given by

$$k_{sat} = \frac{1}{\left(1-\frac{\Gamma_0^2 \ell^4 q_m}{U^2}\right)\left(1-\frac{E_1 \ell}{U}\right)\left(1-\frac{2k^* T}{eU}\right)} \qquad \text{(C.15)}$$

where

$\Gamma_0^2 = (5{,}05 \pm 0{,}25) \times 10^{13}\ \mathrm{V^2 \cdot A^{-1} \cdot m^{-1}}$

ℓ is the chamber depth;

q_m is the measured ionization density $= I/(a\ell)$;

a is the effective collecting electrode area;

U is the absolute value of the collecting voltage;

E_1 $= 4{,}4\ \mathrm{V \cdot m^{-1}}$;

e is the elementary charge;

T is the air temperature, expressed in kelvins;

k^* is the Boltzmann's constant.

When ℓ is expressed in m, I is expressed in A, U is expressed in V, a is expressed in m^2 and T is expressed in K, this correction factor may also be given as

$$k_{sat} = \frac{1}{\left(1-\frac{5{,}05 \times 10^{13} \mathrm{I} \ell^3}{aU^2}\right)\left(1-\frac{4{,}4\ell}{U}\right)\left(1-\frac{17{,}24 \times 10^{-5} T}{U}\right)} \qquad \text{(C.16)}$$

where

the first term in brackets is the volume recombination;

the second term in brackets is the initial recombination;

the last term in brackets is the diffusion.

The total estimated relative uncertainty of k_{sat} is lower than 0,2 % for values of k_{sat} below 1,02, which usually occur in practice.

Table C.1 — Backscatter factors B_{PMMA} and the correction factor k_{ba} for some beta-particle radionuclides

	Radionuclide			
	$^{90}Sr+^{90}Y$	$^{85}Kr,^{204}Tl$	^{147}Pm	^{14}C
B_{PMMA}	1,10	1,10	0,99	0,99
k_{ba}	1,01	1,01	1,00	1,00
Relative standard uncertainty of k_{ba}	0,3 %	0,3 %	0,4 %	0,4 %

Table C.2 — The correction factor k_{br} for some beta-particle sources

	Radionuclide			
	$^{90}Sr+^{90}Y$	$^{85}Kr,^{204}Tl$	^{147}Pm	^{14}C
k_{br}	1,000	1,000	0,990	0,983
Relative standard uncertainty	0,2 %	0,2 %	0,2 %	0,2 %

Table C.3 — Typical values for the parameters for transmission functions for $\alpha = 0°$ [range of applicability is $(\eta_{a,t}\, y_0\, \rho_{a0} + 0{,}000\ 6)$ g·cm^{-2} to $(\eta_{a,t}\, y_0\, \rho_{a0} + 0{,}016\ 7)$ g·cm^{-2}; see Equations C.8 and C.9]

Radionuclide and geometry	Value of the coefficient					
	f_0	f_1 (cm^2 g^{-1})	f_2 (cm^6 g^{-3})	f_3	f_4 (cm^2 g^{-1})	f_5 (cm^4 g^{-2})
^{14}C with no filter at $y_0 = 10$ cm	5,610 ± 0,001	− 229 ± 0,1	− 258 736 ± 240	—	—	—
^{147}Pm with flattening filter at $y_0 = 20$ cm	5,688 ± 0,002	− 174 ± 0,12	− 27 187 ± 59	—	—	—
^{204}Tl with flattening filter at $y_0 = 30$ cm[a]	—	—	—	0,848 ± 0,002	17,3 ± 0,08	− 338,2 ± 0,8
^{85}Kr with flattening filter at $y_0 = 30$ cm[a]	—	—	—	0,813 ± 0,003	20,92 ± 0,16	− 406,9 ± 1,9
$^{90}Sr + ^{90}Y$ with flattening filter at $y_0 = 30$ cm	—	—	—	0,632 ± 0,004	13,86 ± 0,19	− 116,0 ± 2,2
$^{90}Sr + ^{90}Y$ with no filter at $y_0 = 11$ cm	—	—	—	0,795 ± 0,001	14,03 ± 0,07	− 171,5 ± 1,6
$^{90}Sr + ^{90}Y$ with no filter at $y_0 = 20$ cm	—	—	—	0,673 ± 0,002	15,71 ± 0,1	− 152,2 ± 1,6
$^{90}Sr + ^{90}Y$ with no filter at $y_0 = 30$ cm	—	—	—	0,511 ± 0,003	18,27 ± 0,15	− 151,1 ± 1,7
$^{90}Sr + ^{90}Y$ with no filter at $y_0 = 50$ cm	—	—	—	0,163 ± 0,006	21,95 ± 0,2	− 136,0 ± 1,6
$^{106}Ru + ^{106}Rh$ with no filter at $y_0 = 10$ cm	—	—	—	0,844 ± 0,001	11,45 ± 0,06	− 154,7 ± 1,7

[a] For ^{85}Kr and ^{204}Tl the values of the coefficients are applicable from $(\eta_{a,t} y_0 \rho_{a0} + 0{,}001\ 6)$ g cm^{-2} to $(\eta_{a,t} y_0 \rho_{a0} + 0{,}016\ 7)$ g·cm^{-2}. In the range from $(\eta_{a,t} y_0 \rho_{a0} + 0{,}000\ 6)$ g·cm^{-2} to $(\eta_{a,t} y_0 \rho_{a0} + 0{,}001\ 6)$ g·cm^{-2} the transmission factors are constant (1,050 for ^{85}Kr and 1,039 for ^{204}Tl).

Table C.4 — Half-lives of various beta-particle emitting radionuclides

Radionuclide	Half-life
^{14}C	(5 730 ± 40) y
^{147}Pm	(958,2 ± 8) d
^{204}Tl	(1 381 ± 8) d
^{85}Kr	(3 915 ± 3) d
$^{90}Sr + {}^{90}Y$	(10 523 ± 35) d
$^{106}Ru + {}^{106}Rh$	(373,6 ± 15) d

Table C.5 — Coefficients for the calculation of k_{pe}

Radionuclide and geometry	Value of the coefficient		
	f_6	f_7 (mm^{-1})	f_8 (mm^{-2})
^{14}C with no filter at $y_0 = 10$ cm	1,00	0,009 1	$-1{,}29 \times 10^{-3}$
^{147}Pm with flattening filter at $y_0 = 20$ cm	1,00	0,001 95	0
^{204}Tl with flattening filter at $y_0 = 30$ cm	1,00	− 0,003 37	$1{,}50 \times 10^{-3}$
^{85}Kr with flattening filter at $y_0 = 30$ cm	1,00	− 0,003 37	$1{,}50 \times 10^{-3}$
$^{90}Sr + {}^{90}Y$ with flattening filter at $y_0 = 30$ cm	1,00	− 0,007 0	0
$^{90}Sr + {}^{90}Y$ with no filter at $y_0 = 11$ cm	1,00	− 0,004 8	0
$^{90}Sr + {}^{90}Y$ with no filter at $y_0 = 20$ cm	1,00	− 0,004 6	0
$^{90}Sr + {}^{90}Y$ with no filter at $y_0 = 30$ cm	1,00	− 0,004 0	0
$^{90}Sr + {}^{90}Y$ with no filter at $y_0 = 50$ cm	1,00	− 0,003 6	0
$^{106}Ru + {}^{106}Rh$ with no filter at $y_0 = 10$ cm	1,00	− 0,005 0	0

Annex D
(informative)

Example of an uncertainty analysis

It is not practical here to cover an assessment of the uncertainty associated with all the possible scenarios for the determination of absorbed-dose rate in a beta-particle reference radiation field. Instead, a specific example will be given in detail to show the applicability of the method [9,10]. The example to be dealt with is the determination of reference beta-particle absorbed-dose rate from a 3 GBq ^{147}Pm source with an extrapolation chamber equipped with a 7,6 mg cm^{-2} PET window, with ionization currents measured with a high-impedance electrometer operated in the feedback capacitor mode. The magnitudes of the measured currents are such that variations in the leakage current need not be considered. A constant current integration time is also used. In this case, we can remove the constant quantities from the reference absorbed dose equation (Equation 10) and write

$$\dot{D}_{\mathrm{R}\beta} = \dot{D}_{\mathrm{t}}\left(\eta_{\mathrm{PET,t}}\rho_{\mathrm{PET}}d_{\mathrm{PET}}\right) = \frac{\left(\bar{W}_0/e\right)s_{\mathrm{t,a}}Ck_{\mathrm{ba}}k_{\mathrm{br}}k_{\mathrm{el}}k_{\mathrm{in}}k_{\mathrm{hu}}k_{\mathrm{ra}}}{\rho_{\mathrm{a0}}at}\left[\frac{\mathrm{d}}{\mathrm{d}l}\left(\Delta U\right)\right]_{\ell=0} \tag{D.1}$$

where ΔU is the corrected difference in the voltage measured across the electrometer feedback capacitor, given by

$$\Delta U = k_{\mathrm{ad}}\,k_{\mathrm{abs}}\,k_{\mathrm{ac}}\,k_{\mathrm{de}}\,k_{\mathrm{di}}\,k_{\mathrm{pe}}\,k_{\mathrm{sat}}\left(U_2 - U_1\right) \tag{D.2}$$

The measurements and parameters necessary for the determination of reference absorbed-dose rate with an extrapolation chamber are listed in Tables D.1 to D.4. They can roughly be divided into two classes: those which affect the determination of the limiting slope, and those which, at least in the first order, do not. The methods employed to assess the effect, either directly on the absorbed-dose rate, or indirectly on the absorbed-dose rate via the limiting slope, are also shown in these tables. As an example of the use of these methods, a full analysis of the combined standard uncertainty of the measurement of the surface absorbed dose is given in Table D.5. In this table, the standard uncertainty $u(y)$ associated with the estimate of a quantity y is given by

$$u^2\left(y\right) = \sum_{i=1}^{N} u_i^2\left(y\right) \tag{D.3}$$

where

$u_i^2\left(y\right)$ is the contribution to the variance associated with the estimate of y resulting from the standard uncertainty associated with the quantity x_i;

$$u_i\left(y\right) = \left|c_i\right|u\left(x_i\right) \tag{D.4}$$

where

c_i is the sensitivity coefficient, associated with x_i [9]

In the majority of cases encountered in source calibration, the expanded uncertainty of the measurement U, is obtained by multiplying the standard uncertainty of the measurement by a coverage factor k,

$$U = ku\,(y) \tag{D.5}$$

The factor $k = 2$ shall be used for a coverage probability of approximately 95 %.

Table D.1 — Measured quantities which mainly affect only the absorbed-dose rate

Measurand	Estimated relative uncertainty using evaluation method B	Quantities affected	Estimated effect determined from
y_0	0,1 %	$D_{R\beta}$ k_{abs}, k_{di}	$D_{R\beta}$ vs. y_0 Equations C.7, C.13
z	0,1 %	$D_{R\beta}$ k_{ra}	$D_{R\beta}$ vs. z $D_{R\beta}$ vs. z
α	0,06 %	$D_{R\beta}$ k_{pe}	$D_{R\beta}$ vs. α Measurement
$\rho_{PET} d_{PET}$	1 %	$D_{R\beta}$	$D_{R\beta}$ vs. D_t
a	0,07 %	$D_{R\beta}$ k_{sat}, k_{ra}	Equation D.1 Equations C.16, C.4
C	0,1 %	$D_{R\beta}$ k_{sat}	Equation D.1 Equation C.16
T	0,1 %	$D_{R\beta}$ k_{sat}	Equation D.1 Equation C.16

Table D.2 — Parameters which affect only the absorbed-dose rate

Parameter	Estimated relative uncertainty using evaluation method B	Quantities affected	Estimated effect determined from
$\bar{W}_0 / e$	0,2 %	$D_{R\beta}$	Equation D.1
$s_{t,a}$	0,6 %	$D_{R\beta}$	Equation D.1
ρ_{a0}	0,04 %	$D_{R\beta}$	Equation D.1
$\eta_{PET,t}$	1,5 %	$D_{R\beta}$	$D_{R\beta}$ vs. D_t
k_{ba}	0,4 %	$D_{R\beta}$	Equation D.1
k_{br}	0,2 %	$D_{R\beta}$	Equation D.1
k_{el}	0,1 %	$D_{R\beta}$	Equation D.1
k_{in}	< 0,01 %	$D_{R\beta}$	Equation D.1
k_{hu}	0,1 %	$D_{R\beta}$	Equation D.1
k_{ra}	0,5 %	$D_{R\beta}$	Equation D.1

Table D.3 — Measured quantities which mainly affect only the limiting slope

Measurand	Estimated relative uncertainty using evaluation method A	Estimated relative uncertainty using evaluation method B	Quantities affected	Estimated effect determined from
$U_1 - U_2$	0,03 %	0,03 %	I	Equation B.3
T		0,03 %	k_{ad}, k_{sat}	Equations C.5, C.16
p		0,05 %	k_{ad}	Equation C.5
r		0,02 %	k_{ad}, k_{hu}	Equation C.5
ℓ constant offset		0,1 %	limiting slope	Fitting
ℓ gain		0,1 %	k_{ac}, k_{di}, k_{pe}, k_{sat}	Equations C.8, C.13, C.14, C.16
U		1 %	k_{sat}	Equation C.16
$t_m - t_0$		< 0,01 %	k_{de}	Equation C.11

Table D.4 — Parameters which affect the limiting slope

Parameter	Estimated relative uncertainty using evaluation method B	Quantities affected	Estimated effect determined from
f_i	5 %	k_{abs}, limiting slope	Fitting
$\eta_{a,t}$	1,5 %	k_{abs}, limiting slope	Fitting
$t_{1/2}$	0,1 %	k_{de}, limiting slope	Fitting
k_{ad}	0,6 %	I, limiting slope	Fitting
k_{pe}	0,2 %	I, limiting slope	Fitting
k_{sat}	0,2 %	I, limiting slope	Fitting
Γ_0^2	4,95 %	k_{sat}	Equation C.16, fitting
E_1		k_{sat}	Equation C.16, fitting
e	0,000 3 %	k_{sat}	Equation C.16, fitting
k^*	0,3 %	k_{sat}	Equation C.16, fitting

Table D.5 — Combined standard uncertainty (uncertainty budget) **for the determination of surface absorbed-dose rate for a ^{147}Pm source with an extrapolation chamber with an electrometer in the feedback capacitor mode for a fixed integration time**

Part A: $I_{\mathrm{corr}} = I\, k_{\mathrm{ad}}\, k_{\mathrm{abs}}\, k_{\mathrm{di}}\, k_{\mathrm{pe}}\, k_{\mathrm{sat}}\, k_{\mathrm{ac}}\, k_{\mathrm{el}}\, k_{\mathrm{in}}\, k_{\mathrm{de}}$

Quantity	Estimate	Standard uncertainty	Sensitivity coefficient	Contribution to the standard uncertainty
I	304,87 fA	0,5 fA	1,076 6	0,538 fA
k_{sat}	1,005 5	0,002	326,42 fA	0,653 fA
k_{ad}	1,027 5	0,006	319,43 fA	1,917 fA
k_{abs}	1,021	0,008	321,47 fA	2,572 fA
k_{el}	1	0,001	328,22 fA	0,328 fA
k_{in}	1	0,000 1	328,22 fA	0,033 fA
k_{di}	1,005	0,001	326,59 fA	0,327 fA
k_{pe}	1,001 9	0,002	327,60 fA	0,655 fA
k_{ac}	1,013 1	0,001	323,98 fA	0,324 fA
k_{de}	1,000 5	0,001	326,06 fA	0,328 fA
I_{corr}	328,22 fA			3,44 fA

Part B: $\dot{D}_{\mathrm{t}}(0) = s_{\mathrm{t,a}}(\bar{W}_0 / e)k_{\mathrm{br}}\, k_{\mathrm{ba}}\, k_{\mathrm{hu}}\, k_{\mathrm{ra}}\, (\mathrm{d}I_{\mathrm{corr}} / d\ell) / (a \cdot \rho_{\mathrm{ao}})$

Quantity	Estimate	Standard uncertainty	Sensitivity coefficient	Contribution to the standard uncertainty
$s_{\mathrm{t,a}}$	1,124	0,006 7	12,76 μGy·s^{-1}	0,085 μGy·s^{-1}
$\bar{W}_0 / e$	33,83 J C^{-1}	0,068 J·C^{-1}	0,424 μGy C·s^{-1}J^{-1}	0,029 μGy·s^{-1}
a	7,251 cm^2	0,005 cm^2	−1,978 μGy·s^{-1}·cm^{-2}	0,010 μGy·s^{-1}
ρ_{a0}	1,197 4 kg·m^{-3}	0,000 5 kg·m^{-3}	−0,012 μGy·m^3·kg^{-1}·s^{-1}	0,000 μGy·s^{-1}
k_{hu}	1,000	0,001	14,34 μGy·s^{-1}	0,014 μGy·s^{-1}
k_{br}	0,998	0,002	14,37 μGy·s^{-1}	0,029 μGy·s^{-1}
k_{ba}	1,000	0,004	14,34 μGy·s^{-1}	0,057 μGy·s^{-1}
k_{ra}	1,000	0,005	14,34 μGy·s^{-1}	0,072 μGy·s^{-1}
dI_{corr} /d ℓ	3281,25 fA·cm^{-1}	34,59 fA·cm^{-1}	0,004 4 μGy·cm·s^{-1}·fA^{-1}	0,151 μGy·s^{-1}
Result:	14,34 μGy·s^{-1}			0,201 μGy·s^{-1}

The standard uncertainty associated with the measurement result given in the bottom right corner of the table is the root sum square of all the uncertainty contributions in the right column. The final result of this example is given with the reported expanded uncertainty of measurement as:

$$\dot{D}_{\mathrm{t}}\,(0) = (14{,}34 \pm 0{,}4)\ \mu\mathrm{Gy} \cdot \mathrm{s}^{-1} \quad (k = 2)$$

Bibliography

[1] CROSS, W.G., *Phys. Med. Biol*. **13**, p. 611 (1968)

[2] ICRU 56:1997, *Dosimetry of External Beta Rays for Radiation Protection*

[3] BÖHM, J., *The National Primary Standard of the PTB for Realizing the Unit of the Absorbed Dose Rate to Tissue for Beta Radiation*, Report PTB-Dos-13, ISSN 0172-7095 (1986)

[4] BOUTILLON, M., and PERROCHE-ROUX, A.M.,*Phys. Med. Biol*. **32**, p. 213 (1987)

[5] ICRU-31:1979, *Average Energy to Produce an Ion Pair*

[6] BÖHM, J., AMBROSI, P., ANKERHOLD, U., HELMSTÄDTER, K., CHRISTENSEN, P., HELT-HANSEN, J., LARSEN, H., HERBAUT, Y., MARCHETTO, A., CHARLES, M.W., DARLEY, P. and VILLARREAL BARAJAS, J.E., *Dosimetry of weakly penetrating radiation*, Report PTB-Dos-30 (1998)

[7] BÖHM, J. *Phys. Med. Biol*. **25**, p. 65 (1980)

[8] CHRISTENSEN, P., BÖHM, J. and FRANCIS, T.M., *Beta Dosimetry — Fifth information seminar on the radiation protection dosimeter intercomparison programme*, Report EUR 11363 EN, 39 (1987)

[9] GUM:1995, *Guide to the Expression of Uncertainty in Measurement,* first edition, BIPM, IEC, IFCC, ISO, IUPAC, IUPAP, OIML

[10] TAYLOR, B.N. and KUYATT, C.E., *Guidelines for Evaluating and Expressing the Uncertainty of NIST Measurement Results*, NIST Technical Note 1297 (1994)

[11] BLECHSCHMIDT, E., *Präzisionsmessungen von Kapazitäten, Induktivitäten und Zeitkonstanten, 2. Auflage*. F. Verlag & Sohn Verlag, Braunschweig (1956)

[12] SOARES, C.G., *Med. Phys*. **18**, p. 787 (1991)

[13] MARKUS, B.,*Strahlentherapie* **101**, p. 111 (1956)

[14] MURTHY, B.K.S. and BÖHM, J., *Radiat. Prot. Dosim.* **2**, p. 63 (1982)

[15] SCHNEIDER, M., BÖHM, J., HOHLFELD, K. and REICH, H., *Proc. 7th Symposium on Microdosimetry,* 8-12 Sept. 1980, Oxford, UK, Report EUR 7147 DE-EN-FR, 231 (1981)

[16] SCHÜREN, H. and HEINZELMAN, M., *Abschätzung des Photoneneinflusses bei Kalibrierungen am Sekundärnormal für Betastrahlung*, Laborbericht D 2/80 der KFA Jülich GmbH (1980)

[17] BÖHM, J. and SCHNEIDER, M., *Determination of Absorbed Dose Rates with Air-Filled Extrapolation Chamber Dimensions or Low Gas Pressures*, CEC-Report EUR 7365 EN, 190 (1982)

[18] BÖHM, J., *Standardization and Calibration in Beta Dosimetry, Proc. Int. Beta Dosimetry Symposium*, Report NUREG/CP-0050, 73 (1984)

[19] BÖHM, J., ALBERTS, W.G., SWINTH, K.L., SOARES, C.G., MCDONALD, J.C., THOMPSON, I.M.G., KRAMER, H.-M., *Radiat. Prot. Dosim*. **86**, p. 87 (1999)

[20] DRAKE, K.-H. and BÖHM, J., *Automatisierter Meßstand für die Dosimetrie von Betastrahlung*, Report PTB-Dos-19, ISSN 0172-7095 (1990)

[21] AMBROSI, P., BEHRENS, R., BÖHM, J. AND SOARES, C.G., *Calibration and proficiency testing of dosimeters — recent developments in ISO and IEC standards*, Proceedings of the 11th International Radiation Protection Association (IRPA), Madrid (2004)

[22] Evaluated Nuclear Structure Data File, National Nuclear Data Center, Brookhaven National Laboratory, www.nndc.bnl.gov (1998 March 6)

[23] BÖHM, J. *Phys. Med. Biol*. **21**, p. 754 (1976)

[24] HELMSTÄDTER, K., BÖHM, J., CHARTIER, J.-L., CUTARELLA, D., CHAUVENET, B., LECANTE, C., CHRISTENSEN, P. AND FRANCIS, T. M. Intercomparison of extrapolation chamber measurements of the directional absorbed dose rate for ^{204}Tl beta radiation *Rad. Prot. Dosim.* **63**, pp. 293-298 (1996)

ICS 17.240

Price based on 36 pages